PCCP

PAPER

View Article Online
View Journal | View Issue

Cite this: *Phys. Chem. Chem. Phys.*, 2017, **19**, 19360

Structural assignment of small cationic silver clusters by far-infrared spectroscopy and DFT calculations†

Johan van der Tol,‡[a] Dewei Jia,‡[a] Yejun Li,[ab] Valeriy Chernyy,[c] Joost M. Bakker,[c] Minh Tho Nguyen,[d] Peter Lievens[a] and Ewald Janssens*[a]

Received 18th May 2017,
Accepted 27th June 2017

DOI: 10.1039/c7cp03335d

rsc.li/pccp

The structures of small cationic silver clusters Ag_n^+ (n = 3–13) are investigated by comparing measured far-infrared multiple photon dissociation spectra of cluster–argon complexes with the calculated harmonic vibrational spectra of different low-energy structural isomers. A global structure search was carried out using the CALYPSO structure prediction method, after which isomers were locally optimized with the meta GGA functional TPSS. The obtained structures of the cationic silver clusters are mostly consistent with earlier ion mobility measurements and photodissociation spectroscopy studies for Ag_n^+ (n = 3–11) and allowed excluding several structural isomers that were considered in those earlier studies, which illustrates the strength of combining multiple experimental techniques for conclusive structural identification. The growth pattern of the cationic silver clusters is discussed and differences with other cationic coinage metal clusters are highlighted.

1. Introduction

Small silver clusters, composed of only a few silver atoms, are of special interest for photography[1] and catalysis.[2,3] The clusters have a discrete density of states and hence exhibit molecule-like behaviour in their size-dependent electronic and optical properties. Silver nanoclusters showed particularly attractive features as fluorophores when confined in different scaffolds such as DNA oligomers,[4] zeolites,[5] or dendrimers.[6] Their appealing features complement the properties of organic dyes and semiconductor quantum dots.

Finding the most stable geometric structure for a given cluster is a challenging problem that requires pieces of information from both theory and experiment. Structural knowledge is, however, a basic requisite to enhance understanding of the functional properties. Over the years several extensive theoretical studies have been devoted to the structural and electronic properties of small silver clusters,[7,8] and only a small selection is mentioned explicitly here. Chen *et al.* studied neutral Ag_n clusters using density functional theory (DFT) and coupled cluster calculations at the CCSD(T) level to determine the low energy isomers for each cluster size for $n < 20$.[9] Jin *et al.* investigated the global minimum structures of neutral, anionic, and cationic silver clusters up to 16 atoms through DFT calculations at the BP86 level using unbiased structure searching methods.[10] Recently Duanmu and Truhlar performed a systematic computational study of small silver clusters ($n \leq 7$) in different charge states, comparing different exchange–correlation functionals.[11] It was shown that the predictive power of functionals with kinetic density dependence is high. Also, Ferrighi *et al.* studied the relation between the two-dimensional to three-dimensional transition sizes of Ag_n^+ and Ag_n^- and the kinetic energy density of different functionals.[12]

Experimentally, there is not much structural data available for isolated silver clusters. The most direct structural information are from the ion mobility measurements performed by Weis *et al.*, which provide geometric cross sections of Ag_n^+ ($n < 12$).[13] A comparison of their results with cross sections of different calculated structural isomers allowed the identification of the geometric structure of some clusters, but so far a unique identification has not been possible for all sizes. Less direct structural

[a] *Laboratory of Solid State Physics and Magnetism, KU Leuven, Celestijnenlaan 200 D, B-3001 Leuven, Belgium. E-mail: ewald.janssens@kuleuven.be*
[b] *Hunan Key Laboratory of Super Microstructure and Ultrafast Process, School of Physics and Electronics, Central South University, Changsha, Hunan 410083, P. R. China*
[c] *Radboud University, Institute for Molecules and Materials, FELIX Laboratory, Toernooiveld 7c, 6525 ED Nijmegen, The Netherlands*
[d] *Department of Chemistry, KU Leuven, Celestijnenlaan 200 F, B-3001 Leuven, Belgium*

† Electronic supplementary information (ESI) available: Assessment of the accuracy of computational levels on Ag_2 and Ag_3; Ar adsorption sites and energies assessed using different computational levels and the effect of Ar adsorption on the vibrational spectra of $\mathbf{Ag_3^+}$ and $\mathbf{Ag_4^+}$; comparison of the infrared spectra of different structural isomers of Ag_n^+ (n = 10–15) with the experiment. See DOI: 10.1039/c7cp03335d

‡ These authors contributed equally to this work.

information comes from a combination of optical absorption measurements with DFT calculations and from photodissociation and collision induced dissociation experiments.[14–16] Recently, A. Shayeghi *et al.* recorded the optical absorption spectra of size selected $\mathbf{Ag_4}^+$, $\mathbf{Ag_6}^+$, $\mathbf{Ag_8}^+$, and $\mathbf{Ag_{10}}^+$ in a molecular beam.[17–19] These beam depletion experiments helped, in combination with time-dependent density functional theory calculations for different structural isomers and earlier ion mobility data, in obtaining high quality structural information for these sizes. The optical absorption spectra of neutral silver clusters Ag_n with n = 4–14, which were deposited in an argon gas matrix, have shown that the s-electrons are most important for the optical response of the small clusters ($n \leq 8$), while d-electrons play a crucial role for larger clusters.[20]

An approach that has proven to be very powerful for structural identification of clusters in the gas phase is infrared multiple photon dissociation (IRMPD) spectroscopy in combination with DFT calculations.[21,22] This technique, except for the small neutral Ag_3 and Ag_4 clusters,[23] so far has not been applied to study silver clusters.

In this work, we use a combination of infrared multiple photon dissociation spectroscopy experiments on cluster–argon complexes and density functional theory calculations to assign the structures of small cationic silver clusters, Ag_n^+ (n = 3–13). The growth pattern of the clusters is discussed and the differences with other coinage metal clusters are highlighted. In addition, also the effect of argon adsorption on the infrared spectra of the clusters is analyzed and discussed.

2. Methods

2.1 Experimental method

Silver clusters are produced by laser vaporization in a molecular beam setup that is connected to a beam line of the Free Electron Lasers for Infrared eXperiments (FELIX) laboratory.[24] Silver atoms are evaporated by firing the 2nd harmonic of a pulsed Nd-YAG laser at a rectangular pure silver target. A short pulse of helium gas mixed with 0.1% argon carries the evaporated silver atoms into a nozzle, where they lose kinetic energy to this carrier gas and cluster together. A fraction of metal clusters form weakly bound cluster–argon complexes. Cooling this nozzle to a low temperature enhances this process.

After expansion into the vacuum, the molecular beam of clusters is collimated by two skimmers and an aperture of 1 mm diameter and enters an ion extraction zone, where the clusters interact with an intense beam of counter propagating IR laser light from FELIX. This aperture combined with the long Rayleigh length of the FELIX laser assured that all detected clusters have been exposed to comparable laser fluence. FELIX produces light in pulse trains of approximately 10 μs with 1 ns spacing between individual pulses. The bandwidth is near-transform limited and amounts to approximately 0.5% FWHM of the central frequency, which translates to 1 cm^{-1} at 200 cm^{-1}. Pulse energies amount to 2–20 mJ per pulse train, depending on the spectroscopic wavenumber $\tilde{\nu}$; fluences of the loosely focused laser beam in the interaction zone range from 2 to 20 mJ mm^{-2}.

Time-of-flight mass spectrometry is used to monitor the effect of the IR light on the cluster size distribution as a function of the excitation frequency. If the frequency of the IR light is in resonance with one of the vibrational modes of a specific cluster–argon complex and a sufficient number of photons are absorbed, the cluster–argon bond will break. This infrared multiple photon dissociation (IR-MPD) can be detected mass spectrometrically. Indeed, argon detachment from $Ag_nAr_m^+$ implies depletion in the mass spectrum for that cluster–argon complex, and intensity growth for the corresponding bare Ag_n^+ cluster (if m = 1) or the $Ag_nAr_{m-1}^+$ complex (if $m > 1$). The complex depletion intensity depends on the amount of absorbed photons, which in turn depends on the IR absorption cross-section.[25] Operating the IR laser at half the repetition rate (5 Hz) of the cluster production cycle (10 Hz), intensities with I_{ON} and without I_{OFF} laser excitation are compared. The intensities are derived from the corresponding mass spectra by fitting the silver cluster isotope patterns to the measured signal. IR-MPD spectra were recorded for $\mathbf{Ag_3}^+$ to $\mathbf{Ag_{13}}^+$ in the far infrared 80–240 cm^{-1} range. Assuming photon density to be ρ, absorption cross section σ, travel distance d and laser pulse energy E, one obtains

$$I_{ON} = I_{OFF}\exp(-\sigma\rho d) \quad \sigma = \frac{\ln(I_{OFF}/I_{ON})}{\rho d}$$

$$\sigma\left[\mathrm{m}^2\right] \propto \sigma_{exp}\left[\mathrm{J}^{-1}\right] = \frac{\ln(I_{OFF}) - \ln(I_{ON})}{E}$$

For the analysis, the square inverse of the fit uncertainty is used as the standard weight when averaging multiple measurements to obtain σ_{exp} as a function of the spectroscopic wavenumber $\tilde{\nu}$.

2.2 Computational method

The low energy structures of cationic silver clusters, Ag_n^+ with n = 3–13, were explored by DFT, employing the kinetic energy density-dependent Tao–Perdew–Staroverov–Scuseria meta-GGA functional (TPSS)[26] in conjunction with the Def2-TZVP basis sets.[27] The TPSS functional has proven to be accurate for the structural properties of silver clusters in different charge states.[11] Level tests demonstrate the good predictive power of the TPSS/Def2-TZVP method for the silver dimers (see details in the ESI,† Table S1). The experimentally determined stretching mode of $\mathbf{Ag_2}^+$ (136.2 ± 1 cm^{-1})[28] corresponds to the calculated value of 129.0 cm^{-1}. For the neutral Ag_2, the bond length determined by rotational spectroscopy (2.53350(48) Å)[29] agrees well with the calculated value of 2.559 Å and the calculated vibrational mode of 191.0 cm^{-1} is in line with the measured one (192.4 cm^{-1}).[30]

The CALYPSO (Crystal structure AnaLYsis by Particle Swarm Optimization)[31] software package was used in combination with the GAUSSIAN 09 program[32] to search for candidate structures. A difficulty in finding the lowest energy structure is the risk of finding a structure corresponding to a local instead of a global minimum, with a similar structure. Particle swarm optimization overcomes large barriers in the energy landscapes by not

tracking a single guess at the same time, but tracking a whole swarm of guesses instead, at different positions in the problem space. Those then interact with each other in order to accelerate the tried solutions into the global minimum, thereby avoiding being trapped in local minima.[31]

Ar adsorption, which is used in experimental action spectroscopy, may have an effect on the energetic order of the structural isomers. For instance, Ar adsorption was shown to invert the energetic order of the two lowest structural isomers of $Ce_3O_5^+$.[33] In the current work we find computationally that Ar adsorption on a lowest energy planar isomer of $\mathbf{Ag_5}^+$ transforms it into a 3D structure. Moreover, even if the overall structure of a metal cluster is not significantly modified by Ar adsorption, the vibrational modes may be shifted. For example, Fielicke *et al.* measured vibrational frequency shifts of a few cm^{-1} for each additional Ar atom that adsorbed on the neutral silver trimer.[23] Similar effects of noble gas attachment on the vibrational spectra also were observed for small Co_n^+ and Au_n clusters.[34,35] We compared the computed vibrational frequencies of the neutral Ag_3 clusters with those found using IR-MPD spectroscopy by Fielicke *et al.* on Ag_3Ar complexes (113 cm^{-1} and 183 cm^{-1}).[23] At the TPSS/Def2-TZVP level the bare neutral Ag_3 cluster has non-degenerate vibrational modes at 119.7 cm^{-1} and 183.6 cm^{-1}, while the metallic frame of its Ar complex exhibits modes at 122.1 cm^{-1} and 185.2 cm^{-1}.

3. Results

3.1 Silver mass spectrum and infrared depletion spectra

In Fig. 1 a calibrated mass spectrum of the silver clusters and their argon complexes is shown. All peaks are isotopically broadened due to the existence of ^{107}Ag and ^{109}Ag isotopes. Cationic silver clusters with sizes from Ag_3 up to Ag_{18} are shown. The intensity, in particular of the Ar complexes, decreases with size, thus reducing the signal-to-noise ratio of the IR-MPD experiments and limiting this work to sizes up to Ag_{15}. Up to four Ar atoms are adsorbed on the smallest cationic clusters, while the larger ones have at most two adsorbed Ar atoms. The relative intensities of different argon complexes for a given silver cluster, *i.e.* the variation of intensity of $Ag_nAr_m^+$ with m, are important for the interpretation of the IR-MPD spectra. Indeed, if the IR light is in resonance with the vibrational modes of a given cluster–argon complex, argon atoms will detach. The intensity of that cluster–argon complex is thus depleted, which can be used to calculate σ_{exp}. The Ar detachment results in the signal growth of complexes with the same number of silver atoms but less argon, and the apparent σ_{exp} of this smaller complex may thus be negative. Therefore, for $Ag_nAr_m^+$ with $1 \leq m < m_{max}$ both signal growth and depletion may take place for a given excitation frequency, implying that absolute σ_{exp} values for a given size are in the strict sense only meaningful for the complex with the largest amount of argon ($m = m_{max}$). Fortunately, the weak binding of argon seems to have a minor effect on the infrared spectra of the studied silver clusters: the frequencies of the bands are not significantly different for different amounts of Ar on the same silver cluster size.

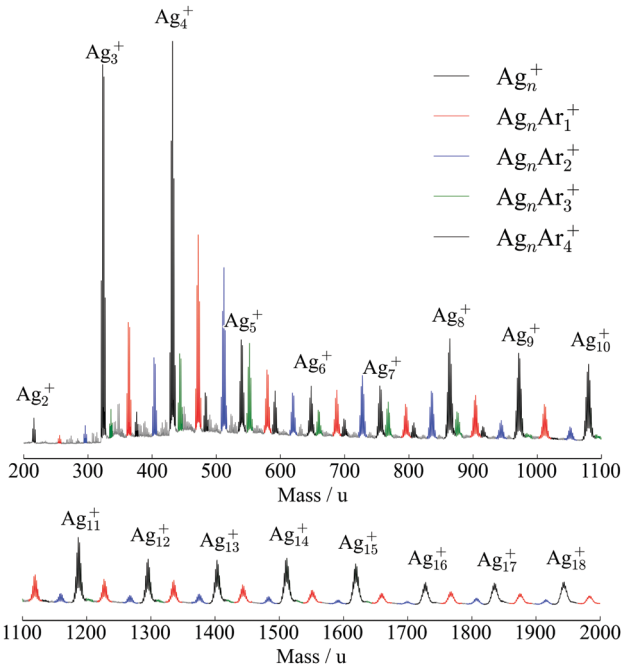

Fig. 1 Mass spectrum of silver clusters and silver–argon complexes in the 200 to 2000 u mass range. The pure Ag_n^+ peaks are labelled. Complexes succeeding the pure clusters containing one, two, three, and four Ar atoms are coloured red, blue, green, and grey, respectively.

This is exemplified for $\mathbf{Ag_3}^+$ and $\mathbf{Ag_4}^+$ in Fig. 2. For example, the depletion at (130.0 ± 0.6) cm^{-1} for $Ag_3Ar_4^+$ corresponds to signal growth at (126.1 ± 0.5) cm^{-1} for $Ag_3Ar_1^+$ and at (129.3 ± 0.5) cm^{-1} for $Ag_3Ar_2^+$. This means that the $\mathbf{Ag_3}^+$ vibrational bands are reproduced in different Ar complexes, which arrive at different times at the detector, thereby demonstrating the overall reproducibility of the measured bands within the experiment itself. The small shifts for different complexes, however, may be related to the effect of Ar adsorption on the metal cluster's vibrational modes.

3.2 Comparison of the IRMPD spectra with simulated spectra for different structural isomers of Ag_n^+

The measured IRMPD spectra of cationic silver cluster-argon complexes are compared with the simulated IR spectra of the lowest energy structural isomers of bare $\mathbf{Ag_3}^+$ and $\mathbf{Ag_4}^+$ as well as their Ar complexes in Fig. 2 and with simulated IR spectra of different structural isomers for $\mathbf{Ag_5}^+$ and $\mathbf{Ag_6}^+$ (Fig. 3), for $\mathbf{Ag_7}^+$ and $\mathbf{Ag_8}^+$ (Fig. 4), for $\mathbf{Ag_{10}}^+$ and $\mathbf{Ag_{11}}^+$ (Fig. 5), and for $\mathbf{Ag_{12}}^+$ and $\mathbf{Ag_{13}}^+$ (Fig. 6). For $\mathbf{Ag_9}^+$ no IRMPD spectra with an acceptable signal-to-noise ratio could be recorded. The isomers shown in the figures are the lowest energy isomers (relative energy to the putative ground state smaller than 0.3 eV).

For $\mathbf{Ag_3}^+$ the IRMPD spectra of the cluster–argon complexes, with one to four attached Ar atoms, all show a single band around 125–130 cm^{-1}. The signal growth or depletion of the band is caused by specific fragmentation channels in which Ar atoms are lost in a successive way. Slight shifts of the measured resonance are likely caused by the minor effect of the argon attachment on the vibrational modes of the metal cluster. The

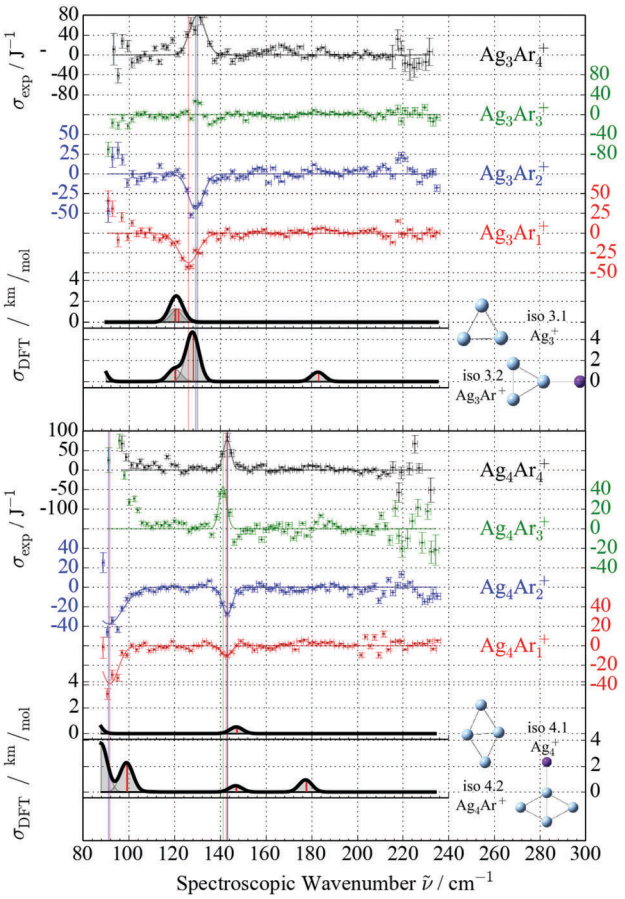

Fig. 2 Comparison of the experimental cross sections (top) of $Ag_3Ar_m^+$ and $Ag_4Ar_m^+$ complexes with calculated harmonic (bottom) infrared spectra of the ground state structures of $\mathbf{Ag_3^+}$ and $\mathbf{Ag_4^+}$, and their Ar complexes Ag_3Ar^+ and Ag_4Ar^+. Top: The negative cross-sections are a consequence of the ingrowth from complexes containing more Ar atoms. If a band reproduces for multiple Ar complexes, this band is fitted with a Gaussian profile. The location is then marked with a vertical line. Bottom: km mol^{-1} is not a unit of σ_{DFT}, but of $\int\sigma_{DFT}\,d\tilde{\nu}$, and corresponds to the height of the vertical red bars, which have been artificially broadened to the light grey areas, and are then convoluted into the black line to allow comparison with experiments.

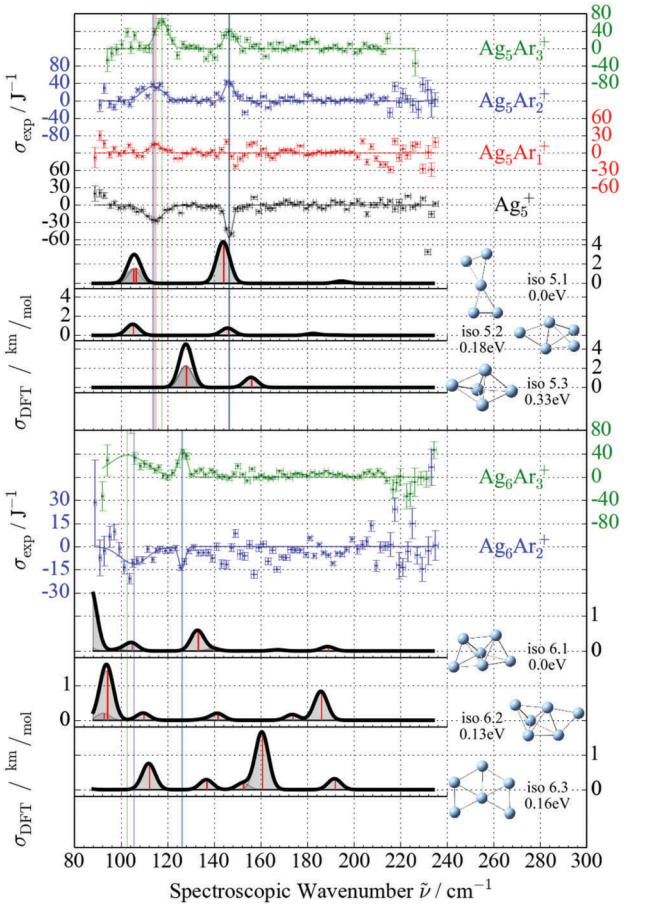

Fig. 3 Comparison of the experimental cross sections of $Ag_5Ar_m^+$ and $Ag_6Ar_m^+$ complexes with calculated harmonic infrared spectra for several structural isomers of $\mathbf{Ag_5^+}$ and $\mathbf{Ag_6^+}$, respectively.

experimental spectra agree with the simulated vibration spectrum of the well-established equilateral triangular structure **iso3.1** of the bare $\mathbf{Ag_3^+}$ cluster.[11,37]

For $\mathbf{Ag_4^+}$ the experiment is in good agreement with the computed harmonic infrared spectrum of the well-established D_{2h} planar rhombic structure **iso4.1**.[13,17,38,39,40]

The effect of argon adsorption on the vibrational spectra of the cationic silver clusters was checked computationally for $\mathbf{Ag_3^+}$ and $\mathbf{Ag_4^+}$ with one or more Ar atoms. Those checks were done at the TPSS/def2 level of theory, at the hybrid TPSSH level, and using the long range corrected LC-wPBE[36] functional in conjunction with larger basis sets. Details are provided in the ESI.†

Here we discuss the effect of Ar attachment at the TPSS/Def2-TZVP level. Upon Ar attachment on $\mathbf{Ag_3^+}$, a new calculated mode appears at 85.4 cm^{-1}, which is a stretching mode of the Ar atom with respect to the $\mathbf{Ag_3^+}$ trimer. In addition, the near-degenerate mode of $\mathbf{Ag_3^+}$ around 120 cm^{-1} splits upon Ar addition to an anti-symmetric stretching mode at 120.0 cm^{-1} and a bending mode at 127.3 cm^{-1} and the symmetric stretching mode around 182.8 cm^{-1} becomes active in Ag_3Ar^+. The degenerate bending mode at 84.0 cm^{-1} in $\mathbf{Ag_4^+}$ splits for Ag_4Ar^+ into two modes at 87.9 and 99.1 cm^{-1}, both of which are a mixture of Ar stretching and cluster bending. These observations are in line with the work of Shayeghi *et al.*, who studied the influence of Ar adsorption on the vibrational spectra of gold, silver, and mixed gold–silver trimers.[37] In that work, the high binding energies of the Ar atoms indicate strong bonds in the Au-rich species; the Ag-rich clusters were shown to be less affected by Ar atoms and behave like the unperturbed clusters surrounded by weakly bound messenger atoms.[37]

Overall these results provide confidence that the calculations at the TPSS/Def2-TZVP level, without inclusion of the Ar messenger atom, are reliable for small silver clusters, with the remark that the calculated vibrational modes, especially the lower frequencies ($\tilde{\nu} < 120$ cm^{-1}), may be shifted relative to the experiment. The results from the current calculations on Ar complexation for $\mathbf{Ag_3^+}$ and $\mathbf{Ag_5^+}$ are consistent with those from Yasrebi and Jamshidi.[44]

The obtained lowest-energy isomer of $\mathbf{Ag_5^+}$, **iso5.1**, has a 3D twisted X-structure. Its harmonic vibrational spectrum shows

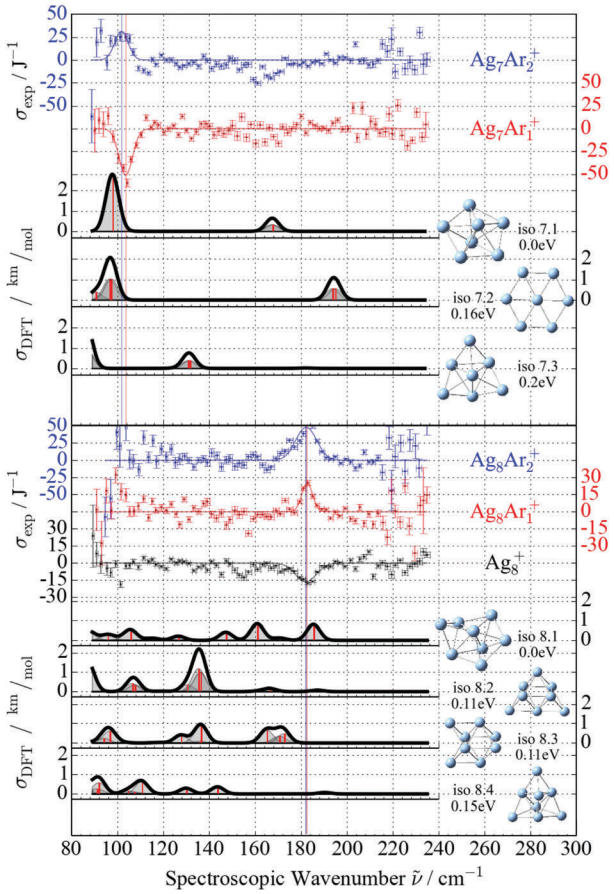

Fig. 4 Comparison of the experimental cross sections of $Ag_7Ar_m^+$ and $Ag_8Ar_m^+$ complexes with calculated harmonic infrared spectra for several structural isomers of **Ag_7^+** and **Ag_8^+**, respectively.

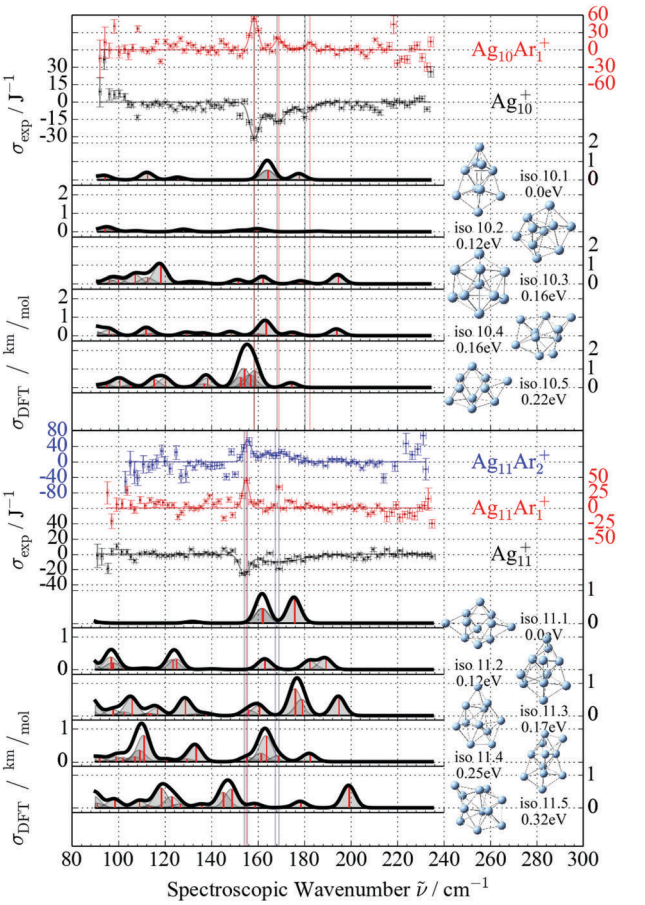

Fig. 5 Comparison of the experimental cross sections of $Ag_{10}Ar_n^+$ and $Ag_{11}Ar_n^+$ complexes with calculated harmonic infrared spectra for several structural isomers of **Ag_{10}^+** and **Ag_{11}^+**, respectively.

good agreement with the experiment, except for a redshift of the lowest observed vibrational mode. Also the infrared spectrum of the second isomer, **iso5.2**, corresponds to the experiment reasonably well, but the relative intensities of the bands do not match and its higher relative energy makes it unlikely that this is the observed isomer in the molecular beam. The infrared spectrum of **iso5.3** does not agree with the experiment. After Ar attachment on **iso5.1** the lower vibrational mode shifts from 106 cm^{-1} to 110.1 cm^{-1} (not shown in figure), which is much closer to the experiment (114 cm^{-1}). Another possible explanation for the slight difference between experiment and computation is the incomplete modelling of the strong anharmonicity of the antisymmetric stretching mode.[38]

For **Ag_6^+**, the $Ag_6Ar_3^+$ complex shows signal depletion at (103 ± 16) cm^{-1} and (126.4 ± 1.2) cm^{-1}, which correspond to the $Ag_6Ar_2^+$ signal growth at (106 ± 7) cm^{-1} and (126.1 ± 1.2) cm^{-1}. The calculated infrared spectrum of **iso6.1**, a bicapped tetrahedron or alternatively a structure composed of three face connected tetrahedra, reproduces both bands of the IRMPD spectra. 3D isomer **iso6.2** and 2D isomer **iso6.3**, an incomplete hexagon, can be ruled out because their intense bands at 185.8 cm^{-1} and 160.4 cm^{-1} are not observed experimentally.

The IRMPD spectra of the Ar complexes of **Ag_7^+** are presented in Fig. 4. The $Ag_7Ar_2^+$ signal is depleted at (102 ± 3) cm^{-1}, which coincides with signal growth for $Ag_7Ar_1^+$ at (103.6 ± 1.1) cm^{-1}. There also is a noisy signal growth around 160 cm^{-1}. Taking into account a small red-shift in the DFT-calculations, the intense band around 100 cm^{-1} is predicted by both **iso7.1**, a pentagonal bipyramid, and **iso7.2**, a hexagonal structure in which the central atom is located slightly out of plane. Since the 190 cm^{-1} band of **iso7.2** is not observed experimentally, **iso7.1** can be identified as the most probable structure in the experiment.

Ag_8^+ has several low-energetic structural isomers. **Iso8.1** is a capped pentagonal bipyramid, which can be constructed from **iso7.1** by capping a triangular face. **Iso8.2** and **iso8.3** are octahedra with two capping atoms at opposite faces on the same and different sides of the square plane, respectively. **Iso8.4** builds on the structural motif of **iso6.1**. The infrared spectrum of **iso8.1** is the only one that reproduces the experimental band at (182 ± 1) cm^{-1}. However, several other (weak) vibrational modes of **iso8.1** are not clearly seen experimentally. Possibly the attached argon causes small shifts of the bands, which could result in the rather noisy experimental spectrum. It should be noted that the cross-section for **Ag_8^+** is consistently lower than zero in the range where the other bands should

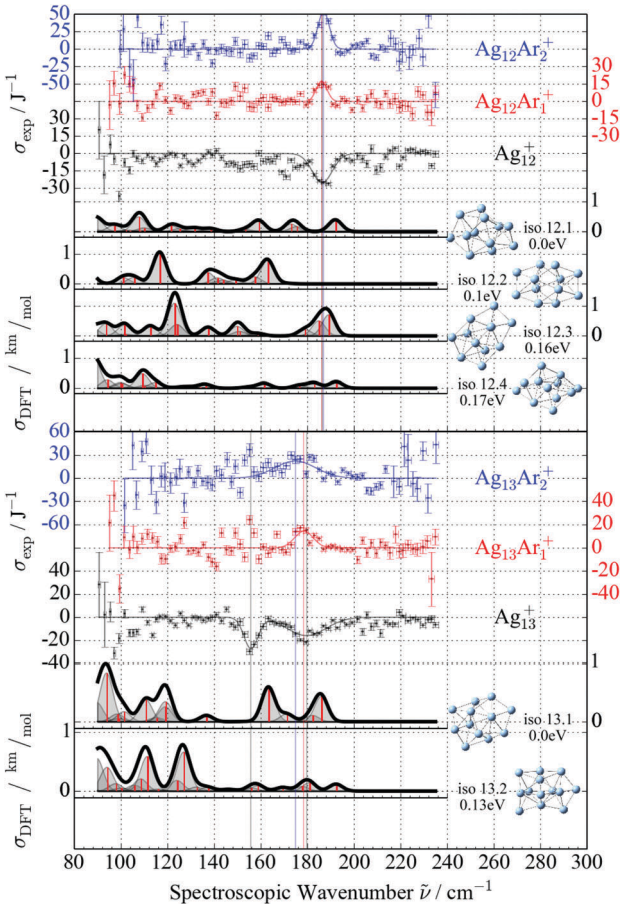

Fig. 6 Comparison of the experimental cross sections of $Ag_{12}Ar_n^+$ and $Ag_{13}Ar_n^+$ complexes with calculated harmonic infrared spectra for several structural isomers of $\mathbf{Ag_{12}}^+$ and $\mathbf{Ag_{13}}^+$, respectively. Note: only structures with relative energies below 0.20 eV are shown.

appear, suggesting depletion of the Ag_8Ar^+ complexes, even though the bands cannot be resolved. Although assignment on the basis of the infrared spectrum alone is inconclusive, we will argue in the discussion section that in combination with available photoabsorption spectroscopy data,[18] **iso8.1** can nonetheless be assigned as the isomer present in the experiment.

For $\mathbf{Ag_9}^+$ no IRMPD spectrum is presented since no bands could be measured with a significant signal-to-noise ratio. The computed lowest-energy isomer is a bicapped pentagonal bipyramid, which builds further on **iso7.1** and **iso8.1**. This growth sequence is continued in $\mathbf{Ag_{10}}^+$, with **iso10.1** having three grouped atoms added to a pentagonal bipyramidal unit. The computed infrared spectrum of **iso10.1** with two close lying high energy bands at 164.0 and 177.5 cm^{-1} agrees well with the vibrational modes in the IRMPD spectrum of $Ag_{10}Ar^+$ at (158.4 ± 0.7) cm^{-1} and (169.0 ± 1.5) cm^{-1}. The infrared spectra of other calculated low-energy isomers do not agree with the experiment.

For $\mathbf{Ag_{11}}^+$ the IRMPD spectrum of the Ar_2 complex is similar to the one of $Ag_{10}Ar^+$ with a double mode at (155.4 ± 1.2) cm^{-1} and (167 ± 4) cm^{-1}, in agreement with the calculated infrared spectrum for **iso11.1** which has bands at 161.8 and 175.5 cm^{-1}.

For $\mathbf{Ag_{12}}^+$ no conclusive assignment can be made on the basis of the infrared spectrum. While the higher energy part of the vibrational spectrum (>140 cm^{-1}) is best reproduced by **iso12.3**, its most intense calculated band at 123.9 cm^{-1} is not seen experimentally. On the other hand, the absence of intense bands below 170 cm^{-1} is well reproduced by **iso12.1**, but this isomer does not provide strong evidence for the most intense experimental band of $Ag_{12}Ar^+$ at (186.1 ± 0.9) cm^{-1}.

$\mathbf{Ag_{13}}^+$ shows a very clear ingrowth at (155.8 ± 1.3) cm^{-1}, although the $Ag_{13}Ar_n^+$ data quality is too low to show the depletion. **Iso13.1** agrees reasonably well with the experiment, but **iso13.3** (+0.22 eV), shown in the ESI,† describes it as well.

4. Discussion

Fig. 7 summarizes the lowest energy structures that were found in this work for Ag_n^+ (n = 3–13). For all of these sizes, except for n = 9 (no experimental spectrum) and for n = 12, the computed harmonic infrared spectra agreed reasonably well with the experimental IRMPD spectra of the corresponding argon complexes. $\mathbf{Ag_3}^+$ adopts a triangular structure, $\mathbf{Ag_4}^+$ a rhombus, and $\mathbf{Ag_5}^+$ a twisted X structure. $\mathbf{Ag_6}^+$ is a bicapped tetrahedron. For the subsequent sizes, the pentagonal bipyramid appears as a structural motif. Facial capping atoms are added to the $\mathbf{Ag_7}^+$ pentagonal bipyramid to form $\mathbf{Ag_8}^+$ and $\mathbf{Ag_9}^+$. In $\mathbf{Ag_9}^+$ the two capping atoms are positioned on two neighbouring faces on the opposite sides of the pentagonal plane. The structure of $\mathbf{Ag_{10}}^+$ builds on that of $\mathbf{Ag_9}^+$ by adding an atom within the pentagonal plane that forms a pyramid with both of the capping atoms. The structural motif changes at $\mathbf{Ag_{11}}^+$, which is based on a triangular prism unit with each face capped by an atom. In $\mathbf{Ag_{12}}^+$ and $\mathbf{Ag_{13}}^+$ again a pentagonal bipyramidal motif can be seen but overall their structures have a low symmetry.

The cationic small silver clusters adopt 2D structures for the smallest clusters $\mathbf{Ag_3}^+$ and $\mathbf{Ag_4}^+$, and transfer to 3D structures at n = 5. This is remarkably different from neutral Ag_n clusters, which have 2D structures for clusters containing up to seven atoms.[11,20] The larger 2D to 3D transition size for neutral than for cationic silver clusters was also found in theoretical work on Cu_n and Pt_n clusters by Chaves *et al.*, who found that the addition of one electron favours more open structures.[41]

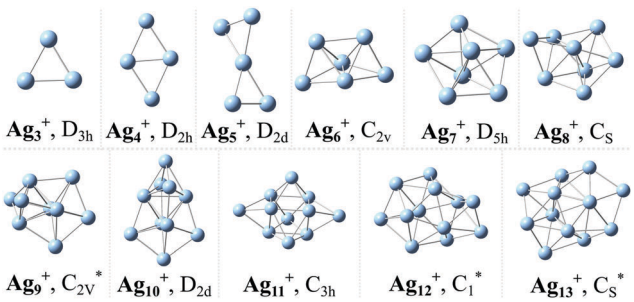

Fig. 7 Global minima isomers for Ag_n^+ (n = 3–13) as obtained by comparison of the simulations with the IRMPD experiments. Those for which the current assignment is not conclusive are indicated with an asterisk.

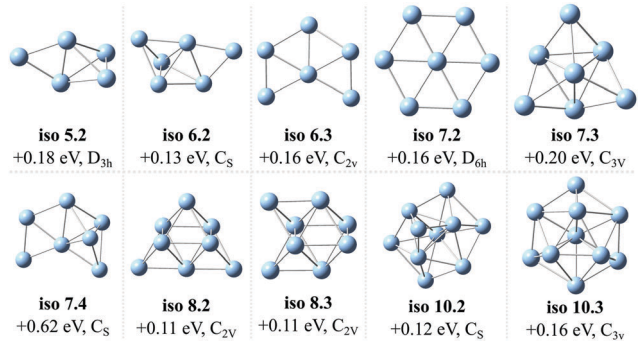

Fig. 8 Competitive isomers of Ag_n^+ (n = 5–9), sorted by increasing energy relative to the global minimum, which can be ruled out because their infrared spectra do not agree with the IRMPD experiments.

Comparing with Au_n^+ and Cu_n^+, Ag_n^+ clusters adopt 3D geometries at the same size (n = 5) as Cu_n^+. This is significantly smaller than that for Au_n^+ clusters, which maintain 2D structures until n = 9,[42] due to the sd electron hybridization caused by significant relativistic effects in Au clusters. Remarkably, the ground state structures found for Ag_n^+ ($n \leq 13$) in the current work have the same symmetry, except for sizes n = 5 and 13, as those found computationally by Chaves *et al.* for Cu_n^+.[41]

Finally, a detailed comparison of the currently obtained structures of small cationic silver clusters is made with structural predictions in the literature. Fig. 8 shows an overview of competitive isomers of Ag_n^+ (n = 5–9), which appear in the literature as candidate lowest-energy structures and effectively can be ruled-out because they are not consistent with the experimental IRMPD spectra.

The comparison of the measured IRMPD spectra with the simulated harmonic infrared spectra confirms the well-established structures for $\mathbf{Ag_3}^+$ and $\mathbf{Ag_4}^+$ in the literature,[11,13,17,37,38] which are an equilateral triangle and a planar rhombic structure, respectively. Also for $\mathbf{Ag_5}^+$ we confirm the twisted X structure of **iso5.1**, which was proposed on the basis of ion mobility measurements.[13] The capped tetrahedron **iso5.2** that was also considered in ref. 13 can be excluded. We also note that a planar isomer with an X structure was found to be a saddle point in our calculations.

The structure of $\mathbf{Ag_6}^+$ was experimentally investigated by ion mobility and photodissociation spectroscopy measurements.[13,18] Both studies point out, in line with computational work,[11] that the bicapped tetrahedral **iso6.1** is the most likely ground state structure. However, also isomer **iso6.2** has an optical absorption spectrum that matches well with the measured photodissociation spectrum[18] and also its measured collision cross section agrees with the calculated value.[13] Since its relative energy is comparable to the accuracy of DFT, the infrared spectrum provides important additional evidence to exclude **iso6.2** and to assign **iso6.1** as the ground state structure of $\mathbf{Ag_6}^+$. This illustrates the strength of combining multiple experimental techniques for conclusive structural identification. The IRMPD experiment on Ar tagged $\mathbf{Ag_7}^+$ clearly assigns the pentagonal bipyramid **iso7.1** as the ground state structure and several low energetic isomers can be excluded in line with the ion mobility experiments by Weis *et al.*[13]

While the earlier ion mobility experiments could not differentiate between **iso8.1**, **iso8.2**, and **iso8.3** for $\mathbf{Ag_8}^+$,[13] the IRMPD spectrum clearly excludes the presence of the last two isomers. This is consistent with the conclusion reached by Shayeghi *et al.*, who combined photodissociation spectroscopy with DFT calculations.[18] The capped pentagonal bipyramid **iso8.1** was also predicted in an *ab initio* study by Bonačić-Koutecký *et al.*[43] Experimentally we could not contribute to the assignment of $\mathbf{Ag_9}^+$, but our computed ground state structure is one of the isomers that had a cross section consistent with the one measured by ion mobility.[13]

Vibrational spectroscopy assigns **iso10.1** as the most stable structure of $\mathbf{Ag_{10}}^+$, while isomers **iso10.2** and **iso10.3** can be excluded. This is consistent with a recent photodissociation spectroscopy experiment in which there was strong evidence that **iso10.1** is the produced isomer.[19] Ion mobility experiments suggested **iso10.3**, but **iso10.1** was not considered in that study.[13] The structure found in the current work for $\mathbf{Ag_{11}}^+$ is consistent with the one proposed on the basis of ion mobility measurements.[13] Finally, no earlier experimental study dealt with the structures of $\mathbf{Ag_{12}}^+$ and $\mathbf{Ag_{13}}^+$.

5. Conclusions

In conclusion, the geometry of small cationic silver clusters, Ag_n^+ (n = 3–13) was studied by a combination of photodissociation spectroscopy experiments on cluster–argon complexes and density functional theory calculations. It was shown computationally that the physisorbed Ar, used as messenger atom in the spectroscopy, had a minor effect on the vibrational frequencies of the silver clusters, but does influence the intensity of some modes. The effect of Ar adsorption on the frequencies is most pronounced for the lower frequency modes, which are slightly blue-shifted upon Ar attachment.

The assigned structures in the present study confirm predictions in the literature on the basis of ion mobility studies and photodissociation experiments, with the remark that by combining the earlier work with the current study, some uncertainty about the structures of $\mathbf{Ag_5}^+$, $\mathbf{Ag_6}^+$, and $\mathbf{Ag_8}^+$ is now resolved. The geometry of $\mathbf{Ag_{12}}^+$ and $\mathbf{Ag_{13}}^+$ was studied for the first time experimentally. Both sizes have a low symmetry structure containing a pentagonal bipyramidal building block. On comparing copper and gold clusters it can be noted that the ground state structures of Ag_n^+ ($n \leq 13$) have the same symmetry, except for sizes n = 5 and 13, as those found for Cu_n^+, while cationic gold clusters maintain 2D structures until n = 9.

Acknowledgements

The authors gratefully acknowledge the Stichting voor Fundamenteel Onderzoek der Materie (FOM) for the support of the FELIX Laboratory and highly appreciate the skilful assistance of the FELIX staff. The research leading to these results has received funding from the European Community's Seventh Framework Programme (FP7/2007-2013) under grant agreement no. 312284.

This work was supported by the Research Foundation-Flanders (FWO/G.0B41.15) and the KU Leuven Research Council (GOA/14/007). D. Jia thanks the China Scholarship Council for financial support (No. 201506290058).

References

1 P. Fayet, F. Granzer, G. Hegenbart, E. Moisar, B. Pishel and L. Wöste, Latent-image generation by deposition of monodisperse silver clusters, *Phys. Rev. Lett.*, 1985, **55**, 3002.
2 G. M. Koretsky and M. B. Knickelbein, The reactions of silver clusters with ethylene and ethylene oxide: Infrared and photoionization studies of $Ag_n(C_2H_4)_m$, $Ag_n(C_2H_4O)_m$ and their deuterated analogs, *J. Chem. Phys.*, 1997, **107**, 10555–10566.
3 L. D. Socaciu, J. Hagen, J. Le Roux, D. Popolan, T. M. Bernhardt, L. Wöste and S. Vajda, Strongly cluster size dependent reaction behavior of CO with O_2 on free silver cluster anions, *J. Chem. Phys.*, 2004, **120**, 2078.
4 T. Vosch, Y. Antoku, J. C. Hsiang, C. I. Richards, J. I. Gonzalez and R. M. Dickson, Strongly emissive individual DNA-encapsulated Ag nanoclusters as single-molecule fluorophores, *Proc. Natl. Acad. Sci. U. S. A.*, 2007, **104**, 12616–12621.
5 O. Fenwick, E. Coutiño-Gonzalez, D. Grandjean, W. Baekelant, F. Richard, S. Bonacchi, D. De Vos, P. Lievens, M. Roeffaers, J. Hofkens and P. Samorì, Tuning the energetics and tailoring the optical properties of silver clusters confined in zeolites, *Nat. Mat.*, 2016, **15**, 1017–1022.
6 J. Zheng and R. M. Dickson, Individual water-soluble dendrimer-encapsulated silver nanodot fluorescence, *J. Am. Chem. Soc.*, 2002, **124**, 13982–13983.
7 R. Fournier, Theoretical study of the structure of silver clusters, *J. Chem. Phys.*, 2001, **115**, 2165–2177.
8 V. Bonačić-Koutecky, V. Veyret and R. Mitrić, Ab initio study of the absorption spectra of Ag_n (n = 5–8) clusters, *J. Chem. Phys.*, 2001, **115**, 10450–10460.
9 M. Chen, J. E. Dyer, K. Li and D. A. Dixon, Prediction of structures and atomization energies of small silver clusters, $(Ag)_n n < 100$, *J. Phys. Chem. A*, 2013, **117**, 8298–8313.
10 Y. Jin, Y. Tian, X. Kuang, C. Zhang and C. Lu, Ab initio search for global minimum structures of pure and boron doped silver clusters, *J. Phys. Chem. A*, 2015, **119**, 6738–6745.
11 K. Duanmu and D. G. Truhlar, Validation of methods for computational catalyst design: Geometries, structures, and energies of neutral and charged silver clusters, *J. Phys. Chem. C*, 2015, **119**, 9617.
12 L. Ferrighi, B. Hammer and G. K. H. Madsen, 2D–3D transition for cationic and anionic gold clusters: A kinetic energy density functional study, *J. Am. Chem. Soc.*, 2009, **131**, 10605–10609.
13 P. Weis, T. Bierweiler, S. Gilb and M. M. Kappes, Structures of small silver cluster cations ($Ag_n^+ n < 12$): Ion mobility measurements *versus* density functional and MP2 calculations, *Chem. Phys. Lett.*, 2002, **355**, 355–364.
14 S. Krückeberg, G. Dietrich, K. Lützenkirchen, L. Schweikhard, C. Walther and J. Ziegler, The dissociation channels of silver clusters Ag_n^+, $3 \leq n \leq 20$, *Int. J. Mass Spectrom. Ion Processes*, 1996, **155**, 141–148.
15 B. A. Collings, K. Athanassenas, D. M. Rayner and P. A. Hackett, Optical spectroscopy of Ag_7, Ag_9^+, and Ag_9. A test of the photodepletion method, *Chem. Phys. Lett.*, 1994, **227**, 490–495.
16 A. Terasaki, S. Minemoto, M. Iseda and T. Kondow, The optical absorption spectrum and photofragmentation processes of silver tetramer ion, *Eur. Phys. J. D*, 1999, **9**, 163–168.
17 A. Shayeghi, R. L. Johnston and R. Schäfer, Evaluation of photodissociation spectroscopy as a structure elucidation tool for isolated clusters: A case study of Ag_4^+ and Au_4^+, *Phys. Chem. Chem. Phys.*, 2013, **15**, 19715–19723.
18 A. Shayeghi, D. A. Götz, R. L. Johnston and R. Schäfer, Optical absorption spectra and structures of Ag_6^+ and Ag_8^+, *Eur. Phys. J. D*, 2015, **69**, 152.
19 A. Shayeghi, R. L. Johnston and R. Schäfer, Global minimum search of Ag_{10}^+ with molecular beam optical spectroscopy, *J. Chem. Phys.*, 2014, **141**, 181104.
20 M. Harb, F. Rabilloud, D. Simon, A. Rydlo, S. Lecoultre, F. Conus, V. Rodrigues and C. Félix, Optical absorption of small silver clusters: Ag_n (n = 4–22), *J. Chem. Phys.*, 2008, **129**, 194108.
21 Y. Li, J. T. Lyon, A. P. Woodham, A. Fielicke and E. Janssens, The geometric structure of silver-doped silicon clusters, *ChemPhysChem*, 2014, **15**, 328–336.
22 E. Janssens, G. Santambrogio, M. Brümmer, L. Wöste, P. Lievens, J. Sauer, G. Meijer and K. R. Asmis, Isomorphous substitution in bimetallic oxide clusters, *Phys. Rev. Lett.*, 2006, **96**, 233401.
23 A. Fielicke, I. Rabin and G. Meijer, Far-infrared spectroscopy of small neutral silver clusters, *J. Phys. Chem. A*, 2006, **110**, 8060–8063.
24 D. Oepts, A. G. F. van der Meer and P. W. van Amersfoort, The free-electron-laser user facility FELIX, *Infrared Phys. Technol.*, 1995, **36**, 297–308.
25 F. Calvo, Y. Li, D. M. Kiawi, J. M. Bakker, P. Parneix and E. Janssens, Nonlinear effects in infrared action spectroscopy of silicon and vanadium oxide clusters: Experiment and kinetic modeling, *Phys. Chem. Chem. Phys.*, 2015, **17**, 25956.
26 J. Tao and J. P. Perdew, Climbing the density functional ladder: Nonempirical meta-generalized gradient approximation designed for molecules and solids, *Phys. Rev. Lett.*, 2003, **91**, 146401.
27 F. Weigend and R. Ahlrichs, Balanced basis sets of split valence, triple zeta valence and quadruple zeta valence quality for H to Rn: Design and assessment of accuracy, *Phys. Chem. Chem. Phys.*, 2005, **7**, 3297–3305.
28 G. I. Nemeth, H. Ungar, C. Yeretzian, H. L. Selzle and E. W. Schlag, High-resolution spectroscopy of Ag_2^+*via* long-lived ZEKE states, *Chem. Phys. Lett.*, 1994, **228**, 1–8.
29 B. Simard, P. A. Hackett, A. M. James and P. R. R. Langridge-Smith, The bond length of silver dimer, *Chem. Phys. Lett.*, 1991, **186**, 415–422.
30 V. Beutel, M. Kuhn and W. Demtröder, Rotationally resolved isotope-selective laser spectroscopy of the Ag_2 molecule, *J. Mol. Spectrosc.*, 1992, **155**, 343–351.

31 Y. Wang, J. Lv, L. Zhu and Y. Ma, CALYPSO: A method for crystal structure prediction, *Comput. Phys. Commun.*, 2012, **183**, 2063–2070.
32 M. J. Frisch, *et al.*, *Gaussian, Inc.*, Wallingford, CT, 2009.
33 A. M. Burow, T. Wende, M. Sierka, R. Wlodarczyk, J. Sauer, P. Claes, L. Jiang, G. Meijer, P. Lievens and K. R. Asmis, Structures and vibrational spectroscopy of partially reduced gas-phase cerium oxide clusters, *Phys. Chem. Chem. Phys.*, 2011, **13**, 19393–19400.
34 R. Gehrke, P. Gruene, A. Fielicke, G. Meijer and K. Reuter, Nature of Ar bonding to small Co_n^+ clusters and its effect on the structure determination by far-infrared absorption spectroscopy, *J. Chem. Phys.*, 2009, **130**, 034306.
35 P. Gruene, D. M. Rayner, B. Redlich, A. F. G. van der Meer, J. T. Lyon, G. Meijer and A. Fielicke, Structures of neutral Au_7, Au_{19}, and Au_{20} clusters in the gas phase, *Science*, 2008, **321**, 674–676.
36 O. A. Vydrov and G. E. Scuseria, Assessment of a long-range corrected hybrid functional, *J. Chem. Phys.*, 2006, **125**, 234109.
37 A. Shayeghi, R. L. Johnston, D. M. Rayner, R. Schäfer and A. Fielicke, The nature of bonding between argon and mixed gold-silver trimers, *Angew. Chem., Int. Ed.*, 2015, **54**, 10675–10680.
38 D. Schooss, S. Gilb, J. Kaller, M. M. Kappes, F. Furche, A. Köhn, K. May and R. Ahlrichs, Photodissociation spectroscopy of $Ag_4^+(N_2)_m m$ = 0–4, *J. Chem. Phys.*, 2000, **113**, 5361–5371.
39 V. Bonačić-Koutecký, J. Burda, R. Mitrić, M. Ge, G. Zampella and P. Fantucci, *J. Chem. Phys.*, 2002, **117**, 3120–3131.
40 E. M. Fernández, J. M. Soler, I. L. Garzón and L. C. Balbás, Trends in the structure and bonding of noble metal clusters, *Phys. Rev. B: Condens. Matter Mater. Phys.*, 2004, **70**, 165403.
41 A. S. Chaves, G. G. Rondina, M. J. Piotrowski, P. Tereshchuk and J. L. F. Da Silva, The role of charge states in the atomic structure of Cu_n and Pt_n (n = 2–14 atoms) clusters: A DFT investigation, *J. Phys. Chem. A*, 2014, **118**, 10813–10821.
42 L. A. Mancera and D. M. Benoit, Vibrational anharmonicity of small gold and silver clusters using the VSCF method, *Phys. Chem. Chem. Phys.*, 2016, **18**, 529–549.
43 V. Bonačić-Koutecký, L. Češpiva, P. Fantucci and J. Koutecký, Effective core potential-configuration interaction study of electronic structure and geometry of small neutral and cationic Ag_n clusters: Predictions and interpretation of measured properties, *J. Chem. Phys.*, 1993, **98**, 7981–7994.
44 S. Yasrebi and Z. Jamshidi, Theoretical investigation of the weak interactions of rare gas atoms with silver clusters by resonance Raman spectroscopy modeling, *Int. J. Quantum Chem.*, 2017, **117**, 15.

